



Review

# Mammalian Sulfatases: Biochemistry, Disease Manifestation, and Therapy

Ryuichi Mashima <sup>1,\*</sup> and Mahito Nakanishi <sup>2</sup>

<sup>1</sup> Department of Clinical Laboratory Medicine, National Center for Child Health and Development, 2-10-1 Okura, Setagaya-ku, Tokyo 157-8535, Japan

<sup>2</sup> TOKIWA-Bio Inc., 2-1-6 Sengen, Tsukuba 305-0047, Japan; nakanishi@tokiwa-bio.com

\* Correspondence: mashima-r@ncchd.go.jp; Fax: +81-3-3417-2238

**Abstract:** Sulfatases are enzymes that catalyze the removal of sulfate from biological substances, an essential process for the homeostasis of the body. They are commonly activated by the unusual amino acid formylglycine, which is formed from cysteine at the catalytic center, mediated by a formylglycine-generating enzyme as a post-translational modification. Sulfatases are expressed in various cellular compartments such as the lysosome, the endoplasmic reticulum, and the Golgi apparatus. The substrates of mammalian sulfatases are sulfolipids, glycosaminoglycans, and steroid hormones. These enzymes maintain neuronal function in both the central and the peripheral nervous system, chondrogenesis and cartilage in the connective tissue, detoxification from xenobiotics and pharmacological compounds in the liver, steroid hormone inactivation in the placenta, and the proper regulation of skin humidification. Human sulfatases comprise 17 genes, 10 of which are involved in congenital disorders, including lysosomal storage disorders, while the function of the remaining seven is still unclear. As for the genes responsible for pathogenesis, therapeutic strategies have been developed. Enzyme replacement therapy with recombinant enzyme agents and gene therapy with therapeutic transgenes delivered by viral vectors are administered to patients. In this review, the biochemical substrates, disease manifestation, and therapy for sulfatases are summarized.

**Keywords:** sulfatase; post-translational modification; formylglycine; biochemistry; gene therapy



**Citation:** Mashima, R.; Nakanishi, M. Mammalian Sulfatases: Biochemistry, Disease Manifestation, and Therapy.

*Int. J. Mol. Sci.* **2022**, *23*, 8153.

<https://doi.org/10.3390/ijms23158153>

ijms23158153

Academic Editor: Alexandre Baykov

Received: 12 June 2022

Accepted: 21 July 2022

Published: 24 July 2022

**Publisher's Note:** MDPI stays neutral with regard to jurisdictional claims in published maps and institutional affiliations.



**Copyright:** © 2022 by the authors. Licensee MDPI, Basel, Switzerland. This article is an open access article distributed under the terms and conditions of the Creative Commons Attribution (CC BY) license (<https://creativecommons.org/licenses/by/4.0/>).

## 1. Introduction

Sulfate is an essential compound for the proper growth and development of living organisms [1]. Its origin is either dietary or through the biosynthesis of sulfur-containing amino acids. The latter process is known as sulfonation and involves 3'-phosphoadenosine 5'-phosphosulfate, a sulfur donor to the substrate, through the enzymatic action of sulfotransferase (Figure 1) [1]. Sulfonation modulates several biological properties of the substrate. First, the sulfonation of carbohydrates leads to glycosaminoglycans with hydrogel-like properties that are necessary for the proper maintenance of cartilage and connective tissues. In the liver, sulfonation detoxifies xenobiotics and certain pharmaceutical compounds, such as acetaminophen or paracetamol, by increasing their hydrophobicity to eliminate them in the urine. Sulfonation also inactivates several biological products induced by hormones and neurotransmitters, maintaining the homeostasis of the body. Thus, improper control of this process disturbs biological systems.

Sulfatases are enzymes that catalyze the removal of sulfate from biological substances. Currently, 17 human sulfatases have been identified (Table 1). These enzymes are activated by the formylglycine-generating enzyme (FGE), which is encoded by the sulfatase modifying factor 1 (*SUMF1*) gene. Importantly, the function of one third of the mammalian sulfatases is currently uncharacterized. Surprisingly, there are over 37,000 sulfatase genes in algae, accounting for approximately 90% of all sulfatase genes in the SulfAtlas Database [2]. Most genes in algae also require FGE as an activator. These sulfatases have two distinct domains: the large N-terminal domain with an alkaline phosphatase-like structure and three

distinct domains, and the smaller C-terminal domain with a four-stranded anti-parallel  $\beta$ -sheet tightly packed against the N-terminal domain through an  $\alpha$ -helix [3]. A few sulfatases present a serine rather than a cysteine at their catalytic center; these are still activated by FGE. Moreover, a limited number of sulfatases that do not require FGE for activation has been reported.

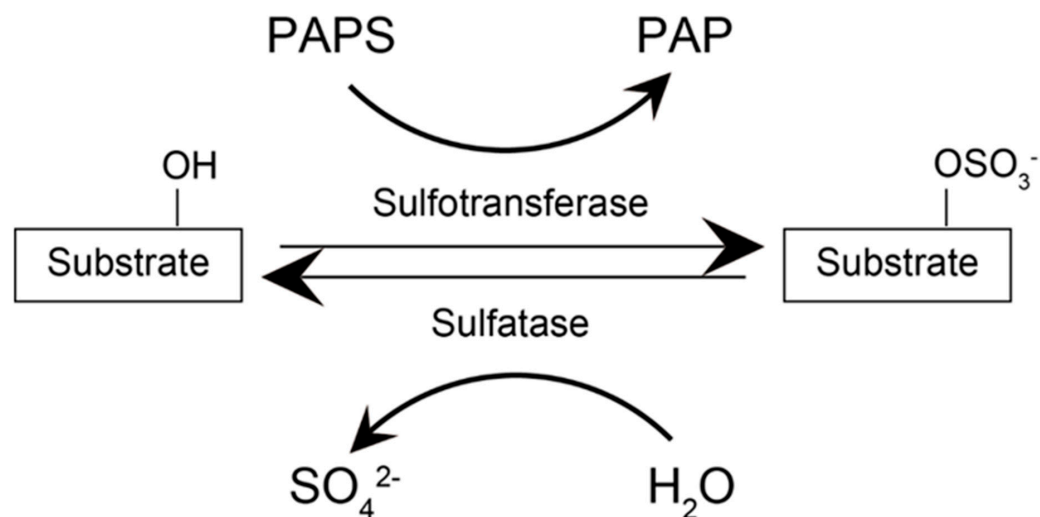


**Figure 1.** Sulfatase and sulfotransferase. Sulfotransferase transfers a sulfate at the expense of PAPS at the specific position of lipids, cholesterol, and sugars. Sulfatase removes a sulfate from the substrate. Sulfatase needs to be activated by a formylglycine-generating enzyme, as described in the text. PAPS, 3'-phosphoadenosine 5'-phosphosulfate.

**Table 1.** Sulfatases in humans and mice.

| Sulfatase                           | Human Gene       | OMIM   | Genetic Disorder                           | Mouse Gene     | Phenotype   | Ref. |
|-------------------------------------|------------------|--------|--|----------------|---|------|
| Arylsulfatase A                     | <i>ARSA</i>      | 250100 | Metachromatic leukodystrophy (MLD)         | <i>Arsa</i>    | CNS and PNS involvement                               | [4]  |
| Arylsulfatase B                     | <i>ARSB</i>      | 253200 | Maroteaux–Lamy syndrome (MPS VI)           | <i>Arsb</i>    | Bone deformity, visceral manifestation                | [5]  |
| Arylsulfatase C (Steroid sulfatase) | <i>ARSC, STS</i> | 308100 | X-linked ichthyosis (XLI); difficult labor | <i>Arsc</i>    | Not reported  |      |
| Arylsulfatase D                     | <i>ARSD</i>      | 300002 | Not reported                               | Not identified | Not applicable  |      |
| Arylsulfatase E                     | <i>ARSE</i>      | 302950 | Chondrodysplasia punctata 1 (CDPX1)        | <i>Arse</i>    | Not reported  |      |
| Arylsulfatase F                     | <i>ARSF</i>      | 300003 | Not reported                               | Not identified | Not applicable  |      |
| Arylsulfatase G                     | <i>ARSG</i>      | 618144 | Usher syndrome type IV                     | <i>Arsg</i>    | Neuronal cell death and behavioral deficits           | [6]  |
| Arylsulfatase H                     | <i>ARSH</i>      | 300586 | Not reported                               | Not identified | Not applicable  |      |
| Arylsulfatase I                     | <i>ARSI</i>      | 610009 | Not reported                               | <i>Arsi</i>    | Not reported  |      |
| Arylsulfatase J                     | <i>ARSJ</i>      | 610010 | Not reported                               | <i>Arsj</i>    | Not reported  |      |
| Arylsulfatase K                     | <i>ARSK</i>      | 610011 | Mucopolysaccharidosis type 10              | <i>Arsk</i>    | Mild behavioral changes                               | [7]  |
| Galactosamine 6-sulfatase           | <i>GALNS</i>     | 253000 | Morquio A syndrome (MPS IVA)               | <i>Galns</i>   | Bone deformity, visceral manifestation                | [8]  |
| Glucosamine 6-sulfatase             | <i>GNS</i>       | 252940 | Sanfilippo D syndrome (MPS IIID)           | <i>Gns</i>     | CNS phenotype, visceral manifestation                 | [9]  |
| Heparan N-sulfatase (sulfamidase)   | <i>SGSH</i>      | 252900 | Sanfilippo A syndrome (MPS IIIA)           | <i>Sgsh</i>    | CNS phenotype, visceral manifestation                 | [10] |
| Iduronate 2-sulfatase               | <i>IDS</i>       | 309900 | Hunter syndrome (MPS II)                   | <i>Ids</i>     | CNS phenotype, bone deformity, visceral manifestation | [11] |

**Table 1.** *Cont.*

| Sulfatase   | Human Gene   | OMIM   | Genetic Disorder | Mouse Gene   | Phenotype   | Ref. |
|-------------|--------------|--------|------------------|--------------|---|------|
| Sulfatase 1 | <i>SULF1</i> | 610012 | Not reported     | <i>Sulf1</i> | Short life span, skeletal and renal abnormalities | [12] |
| Sulfatase 2 | <i>SULF2</i> | 610013 | Not reported     | <i>Sulf2</i> | Short life span; skeletal and renal abnormalities | [12] |

OMIM, Online Mendelian Inheritance in Man.

## 2. Biochemistry

Sulfatases remove sulfate from a substrate (Figure 1). Mammalian sulfatases have a broad substrate specificity (Table 2). Iduronate 2-sulfatase (IDS), arylsulfatase B (ARSB), glucosamine 6-sulfatase (GNS), heparan N-sulfatase (sulfamidase, SGSH), arylsulfatase G (ARSG), and galactosamine 6-sulfatase (GALNS) remove  $\text{SO}_4^{2-}$  with glycosaminoglycans such as dermatan sulfate (DS), heparan sulfate (HS), and keratan sulfate. More specifically, IDS and ARSB react with DS by removing 2-O-sulfate and 6-O-sulfate, respectively. IDS, SGSH, GNS, and ARSG react with HS by removing 2-O-sulfate, N-O-sulfate, 6-O-sulfate, and 3-O-sulfate, respectively. GALNS removes 6-O-sulfate from keratan sulfate. In contrast, arylsulfatase A (ARSA) and arylsulfatase C (ARSC) react with non-carbohydrate compounds: ARSA reacts with sulfolipids, and ARSC reacts with 3-O-steroids. Currently, the substrate for arylsulfatase E (ARSE) remains uncharacterized. Although the specificity of substrates varies, the amino acid sequences of the catalytic center are well-conserved with a consensus sequence of (C/S)XPSRXXX(L/M)TG(R/K/L) [13], where C is the target cysteine residue to be converted into formylglycine. The proposed mechanisms involve the addition of an oxygen atom to the cysteine, which is activated by Cu (I) with two cysteine residues [14]. The flavin-adenine dinucleotide-containing proteins Erv2p and Ero1p have been suggested as electron donors of this redox reaction [13].

**Table 2.** Subcellular localization and substrate of sulfatases.

| Sulfatase    | Subcellular Localization | Substrate   |
|--------------|--------------------------|---|
| <i>ARSA</i>  | Lysosome                 | Sulfatide   |
| <i>ARSB</i>  | Lysosome                 | 4-O; DS   |
| <i>ARSC</i>  | ER/microsome             | DHEAS, estriol sulfate, pregnolone sulfate, cholesterol sulfate |
| <i>ARSD</i>  | ER                       | Uncharacterized   |
| <i>ARSE</i>  | Golgi                    | Uncharacterized   |
| <i>ARSF</i>  | ER                       | Uncharacterized   |
| <i>ARSG</i>  | Lysosome                 | 3-O; HS   |
| <i>ARSH</i>  | Uncharacterized          | Uncharacterized   |
| <i>ARSI</i>  | Uncharacterized          | Uncharacterized   |
| <i>ARSJ</i>  | Uncharacterized          | Uncharacterized   |
| <i>ARSK</i>  | Uncharacterized          | 2-O; HS, CS   |
| <i>GALNS</i> | Lysosome                 | 6-O; KS, CS   |
| <i>GNS</i>   | Lysosome                 | 6-O; HS   |
| <i>SGSH</i>  | Lysosome                 | N-O; HS   |
| <i>IDS</i>   | Lysosome                 | 2-O; DS/HS  |
| <i>SULF1</i> | Extracellular            | 6-O; HS   |
| <i>SULF2</i> | Extracellular            | 6-O; HS   |

DHEAS, dehydroepiandrosterone sulfate.

Based on biochemical data, the preferable substrate of FGE in vitro is ARSA (Table 2) [13]. Similarly, ARSB is another good substrate for FGE. The reactivity for ARSE is higher than that for ARSA. Conversely, SGSH, GALNS, and IDS are poor substrates compared to ARSA. However, it is important to remember that this assay measures the reactivity of

FGE to the corresponding 23-mer peptides of sulfatases; thus, the results only warrant the biochemical reaction. To consider the physiological enzyme activity of sulfatases based on FGE-mediated activation, it is also important to consider the expression levels of FGE within specific tissues. An initial characterization of FGE revealed that this enzyme is highly expressed in the kidney and scarcely expressed in the brain [15].

In the fetal brain, nine sulfatases are abundantly expressed, with a rather broad range of substrate specificity [1]. Among them, the *IDS*, *GNS*, *ARSB*, *ARSK*, *SULF1*, and *SULF2* genes, which are responsible for proteoglycan metabolism, are highly expressed. Furthermore, the *ARSA* gene that codifies a key enzyme for the maintenance of myelination in the nerve system is also highly expressed. The *ARSC* gene, also known as the steroid sulfatase (*STS*) gene, essential for X-linked ichthyosis (XLI) of the skin and the codification of an enzyme involved in steroid metabolism by catalyzing 3-O-sulfate removal, is also highly expressed. Except for the *STS* gene, the remaining sulfatase genes are expressed in the cerebrum, brain stem, diencephalon, and cerebellum parts of the brain throughout the 4–17 weeks of the gestational period. The *ARSC* mRNA levels are low in the cerebrum when compared to the other three regions, suggesting that steroid activity is spatially confined to the latter three brain regions during early neurodevelopment. The *SULF1* and *SULF2* mRNA levels are high in the developing fetal brain. They lead to the production of an enzyme that removes 6-O-sulfate from proteoglycans extracellularly and modulates the gradient of the morphogen *Shh* during embryonic development. The same study also showed that *SUMF2* had higher expression than *SUMF1*, raising the possibility that both enzymes cooperatively regulate sulfatase activity in the brain. The short bursts of increased mRNA expression of *ARSI*, *GALNS*, and *SGSH* suggest a localized and temporary requirement for proteoglycan-metabolizing sulfatases. The abundant mRNA expression of these sulfatases implies that the metabolism of sulfur-containing substances is an active process in the developing fetal brain.

### 3. Disease Manifestations and Phenotypes in Animal Models

Mucopolysaccharidoses (MPSs) are a group of congenital disorders presenting an accumulation of mucopolysaccharides, such as DS, HS, keratan sulfate, and chondroitin sulfate [16]. Visceral manifestations are widely prevalent in MPSs. Additionally, HS accumulation caused by a deficiency of *IDS* (MPS II), *SGSH* (MPS IIIA), and *GNS* (MPS IIID) is related to neurological manifestations, such as cognitive decline. In contrast, DS accumulation is associated with a deficiency of *IDS* (MPS II) and *ARSB* (MPS VI), leading to skeletal manifestations such as short stature, increased head circumference, claw hand, and coarse facial features. MPS IVA is caused by a deficiency of *GALNS* that affects the bones and the heart. Interestingly, the affected individuals show normal growth at birth, presenting these developmental defects only at age 4–5.

Metachromatic leukodystrophy (MLD) is caused by a failure of myelination homeostasis by a deficiency of the *ARSA* enzyme in the central (CNS) and the peripheral (PNS) nervous system, leading to demyelination and, consequently, devastating neural manifestations. The disease subtypes are defined by the age of onset and are categorized into infantile-, juvenile-, and adult-onset. Patients with infantile-onset MLD, the most severe subtype, show symptoms within the first two years of life and decease within a few years [17].

Chondrodysplasia punctate 1 is caused by a pathogenic mutation in the *ARSE* gene that causes short stature and the calcification of the epiphyseal cartilage and its neighboring area [18]. XLI, also known as steroid sulfatase deficiency, is caused by a pathogenic mutation in the *ARSC* gene, leading to skin disorders [19,20]. A deficiency of the *ARSC* gene results in an abnormal accumulation of cholesterol 3-O-sulfate, leading to a loss of proper moisture of the skin. A deficiency of the *STS* enzyme in the placenta causes difficulties in labor due to a limited accumulation of the hormone dehydroepiandrosterone sulfate.

Lysosomal storage disorders (LSDs) are congenital disorders characterized by an accumulation of specific metabolites that are degraded by lysosomes [21]. Approximately

50 genes are implicated in various LSDs, including MPSs, sphingolipidoses, neuronal lipofuscinosis, and glycogen storage disorders; additionally, other genes are related to lysosomal biogenesis, membrane proteins with transporter function, and enzymes responsible for the maturation of LSD-involved enzymes. Major phenotypes of LSDs include neuronal, skeletal, and visceral manifestations that emerge at earlier ages. Among the aforementioned disorders, MPS and MLD are included in LSDs.

The phenotypes for Sulf1/Sulf2 have been also described in animal models. These enzymes locate extracellularly to remove a sulfate at the 6-O position of GlcNAc at a neutral pH. A deficiency of these enzymes leads to embryonic development and the chondrogenic phenotype. In Sulf1(-/-) mice, the differentiation of neural progenitors to neurons is enhanced.

#### 4. Treatment Strategies

In the context of treatment, pathogenic cells need to be restored to the original non-pathogenic conditions. To achieve this, a variety of strategies have been developed. Enzyme replacement therapy provides therapeutic enzymes to the cells, while gene therapy transduces cDNA to the pathogenic cells. Hematopoietic stem cell transplantation exerts its therapeutic effects by transplanting hematopoietic stem cells that generate mature cells, such as lymphocytes, erythrocytes, platelets, and other myeloid cells. Additionally, pharmacological chaperons that are low-molecular-weight compounds play a substantial role in correcting dysfunctional pathogenic enzymes.

Cross-correction is an important mechanism for the regulation of enzymes related to LSDs. LSD-related enzymes target the lysosome via the mannose-6-phosphate-mediated intracellular traffic mechanism, while exogenously administered enzymes also reach lysosomes by this mechanism. This implies that bone marrow transplants, enzyme replacement therapy, and gene therapy do not necessarily transduce therapeutic cDNA into the pathogenic cells. Alternatively, once these active enzymes are expressed in the cells adjacent to the pathogenic cells, the treatment effect is exerted by cross-correction.

##### 4.1. Enzyme Replacement Therapy

Enzyme replacement therapy was initially developed for Gaucher disease and was then applied to other LSDs. Although, in the early phase, therapeutic enzymes were purified from the placenta, currently the available commercial products are produced under controlled conditions and with an authorized procedure. Therapeutic enzymes are usually administered fortnightly to treat visceral symptoms. Currently, the treatment of CNS manifestations is the focus of research. To achieve this, a variety of delivery protocols other than intravenous administration, e.g., intrathecal administration [22], have been developed. Moreover, a method to efficiently transduce enzyme agents to the brain has been developed with an enzyme agent fused to the Fab domain of the anti-human transferrin receptor of the enzyme's N-terminal [23]. Another enzyme agent that links to the Fc domain of the monoclonal anti-human transferrin receptor antibody through the enzyme's C-terminal has been also developed [24].

##### 4.2. Gene Therapy

Gene therapy is an emerging technique through which a transgene is delivered into the body by viral-vector-mediated technology. Compared to enzyme replacement therapy, which requires regular administration, gene therapy is considered a one-time therapy that relieves patients from frequent medical visits.

###### 4.2.1. Adeno-Associated Virus (AAV)

AAV is a widely used vector for gene therapy [25]. AAV was originally discovered as an associated virus of adenoviruses more than five decades ago. AAV is a family of parvoviruses that infect humans with unknown pathogenicity. Therapeutic AAV carries transgenes of up to approximately 5.5 kb. There are many serotypes with different tropisms.

For example, AAV9 infects neural cells, whereas AAV2 infects the liver. Additionally, in many hybrid AAVs, the serotypes of the capsid and the cloning vector are different. The tropism depends on the amino acid sequence of capsid proteins. It has been demonstrated that the replacement of tyrosine with phenylalanine dramatically increases the efficiency of AAV transduction [26]. Usually, viral particles are prepared by transfecting three plasmids that express cDNA (a cloning vector), capsid proteins, and a replicase enzyme. For further purification, the produced AAV particle is isolated using ultracentrifugation and/or ion exchange chromatography. In addition to no severe adverse events, the biosafety of AAV has also been extensively studied in many non-human primate models [27].

For improved therapeutic outcomes, the administration of a larger amount of AAV particles is needed; however, this occasionally leads to hepatic toxicity. To reduce the amount of the vector, Stristava et al. [26] replaced threonine with phenylalanine in the capsid protein VP-3, leading to enhanced AAV stability. Regarding the production of gene-delivery medicines at a large scale, ultracentrifugation using cesium chloride limits the capacity of sample processing. Hence, this technique has been replaced by the iodixanol-mediated protocol [25]. Based on these technical improvements, AAV has been established as a therapeutic agent for gene therapy.

#### 4.2.2. Lentiviral Vector (LV)

LV is another viral vector widely used in therapeutics and for ex vivo gene transduction [28]. LV originated from the HIV-1 virus and was then developed into a non-self-replicating viral vector. Currently, the available plasmid system uses three plasmids, namely, the transgene, helper, and capsid plasmids. Third-generation vectors lack accessory genes and part of the native U3 promoter. Apart from these advances, gene therapy researchers investigate more adequate promoters, modifiers, and the 3'-UTR region that may enhance the stability of the transcript [29]. Despite the possibility of multiple applications, LV-mediated gene therapy is mostly used for autologous transplantation. Thus, if the medical facility where the procedure takes place is not easily accessible to the patient, this may be problematic. Currently, research on the efficient transportation of gene-transfected cells is under examination. Apart from LSDs, the use of LV in immunology and oncology has been growing. For instance, chimeric antigen receptor-T therapy delivers a modified receptor specific to antigens against pathogenic T cells.

### 5. Gene Therapy for Sulfatases

Among the 17 human sulfatases, *ARSA*, *ARSB*, *GALNS*, *GNS*, *SGSH*, and *IDS* are involved in LSDs for which gene therapy studies have been performed (Table 1). Here, we present a summary of the current status of relevant preclinical and clinical research. Some unique issues, such as the phenotype of the disorder and the choice of AAV serotype, animal models, and vector organization, are also described.

#### 5.1. ARSA

ARSA is an enzyme responsible for MLD (OMIM 250100). MLD is a detrimental disorder that affects both the CNS and PNS. Compared to other LSDs, MLD is the best-studied sulfatase deficiency for gene therapy (Table 3). A pilot study of newborn screenings for MLD has been reported [30]. In this context, the substrate for the measurement of ARSA's enzymatic activity in dried blood spots by liquid chromatography–tandem mass spectrometry has been developed [31].

Ex vivo gene therapy for MLD is a success in this field (reviewed in [28]). Although *Arsa*-deficient mice exhibit milder phenotypes than humans, impaired neurophysiology, rotarod latency, and behavioral data were documented at 6 months of age compared to age-matched controls [4,31]. LV-mediated hematopoietic stem-cell gene therapy in *Arsa*-deficient mice showed a supraphysiological ARSA enzyme activity in the liver and peripheral blood and a marginal elevation in the brain [4]. In detailed histological analyses, the reduced number of neurons in *Arsa*-deficient mice in the CA2/3 region of the hip-

pocampus and the Purkinje cell layer of the cerebellum was reversed by LV-mediated gene therapy. The results of subsequent clinical studies revealed that the MRI evaluation was improved [17,32,33]. In the first report of a relevant clinical study [31], (i) the vectors were manufactured with authorized protocols, (ii) the vector copy number reached acceptable levels for treatment, (iii) an improved MRI evaluation of the brain was observed, and (iv) the integration sites of the vector in the chromosomes identified in three patients were similar to LV-treated patients with X-linked adrenoleukodystrophy with a partially overlapping pattern. Consequently, the LV-based therapeutic agent Libmeldy was approved by the European Medical Agency and is now commercially available by Orchard Therapeutics, London, UK.

Gene therapy for MLD started with AAV-mediated transduction (Table 3). Numerous animal studies established that an AAV-mediated enhancement of ARSA enzyme activity is beneficial. Importantly, the discussion related to the delivery or the site of infusion is ongoing. An initial attempt suggested the intravenous injection of AAV. In the case of MLD, various injection sites in the brain have been examined. Because the administered AAV stays at or near the site of injection and fails to easily diffuse, an altered injection protocol for the brain should be developed.

ARSA is a lysosomal sulfatase that is activated by multiple steps in the cells. After translation in the endoplasmic reticulum, the immature protein first passes through the Golgi apparatus, where the cysteine at the catalytic center is converted to formylglycine by the enzymatic action of FGE [34]. Failure in this process leads to multiple sulfatase deficiency, a known LSD with an elevation of all LSD-related sulfatases. In the context of gene therapy, the maximization of enzyme activity needs to be pursued. For this, the role of the *SUMF1* gene has been investigated in vitro and in vivo. The simultaneous expression of both *ARSA* and *SUMF1* bicistronically [35] or a vector system containing a mixture of *ARSA* and *SUMF1* [36] were examined. In both cases, enhanced *ARSA* gene expression was observed.

## 5.2. ARSB

ARSB is an enzyme responsible for MPS type VI (MPS VI: OMIM 253200), with elevated DS levels in the body being a hallmark of the disease. The major manifestation involves skeletal deformity, while no CNS effects have been observed. Even though the disease is global, many patients are located in northeastern Brazil [90]. The hybrid vector AAV2/8 was used in a preclinical study to target the skeletal tissue of the body. To examine the proper site of injection and the amount of vector, the efficacy of therapy, the safety profile of the vector, and other preclinical parameters, many animal models were used, including rats, cats, and mice. Animal models other than mice were also used to study other sulfatases of LSDs [91] because of their size.

## 5.3. GALNS

GALNS is an enzyme responsible for MPS type IVA (MPS IVA: OMIM 253000), also known as Morquio A syndrome. Its major symptoms are manifested in the bones and the visceral organs but not in the CNS. In an animal study, the tested AAV8-based vector provided prolonged expression of GALNS enzyme activity for over 6 months after administration, ameliorating the accumulation of keratan sulfate and improving a variety of pathological markers in the growth plate and the articular disc of the knee joint as well as the valve and muscle of the heart [59].

**Table 3.** Vectors used for the study of sulfatase gene therapy.

| Sulfatase | Disorder | Year | Vector    | Promoter      | Transgene | 3'-UTR | Animal | Dose                                      | Route                        | Ref                               |             |
|-----------|----------|------|-----------|---------------|-----------|--------|--------|---|------------------------------|-----------------------------------|-------------|
| ARSA      | MLD      | 2006 | AAV5      | PGK           | ARSA      | WPRE   | Mouse  | $3 \times 10^9$ particles                 | Brain                        | [37]                              |             |
|           |          | 2009 | AAV1      | CAG           | ARSA      |        | Mouse  | $5 \times 10^{10}$ particles              | Intrathecal                  | [38]                              |             |
|           |          | 2012 | AAVrh     | CAG           | ARSA      |        | Mouse  | $2.3 \times 10^9$ vg                      | Intravenous                  | [39]                              |             |
|           |          | 2012 | AAV5      | PGK           | ARSA      |        | Mouse  | $2.3 \times 10^9$ vg                      | Intravenous                  | [39]                              |             |
|           |          | 2014 | AAVrh10   | CMV           | ARSA      |        | NHP    | $1.5 \times 10^{12}$ gc                   | Brain                        | [40]                              |             |
|           |          | 2014 | ssAAV9    | Not described | ARSA      |        | Mouse  | $2 \times 10^{12}$ vg                     | Intravenous                  | [41]                              |             |
|           |          | 2015 | AAV1      | CAG           | ARSA      |        | Mouse  | $2.3 \times 10^{11}$ vg                   | Brain                        | [42]                              |             |
|           |          | 2015 | AAV9      | CAG           | ARSA      |        | Mouse  | $1.1 \times 10^{10}$ vg                   | Brain                        | [42]                              |             |
|           |          | 2015 | scAAV1    | CAG           | ARSA      |        | Mouse  | $1.1 \times 10^{10}$ vg                   | Brain                        | [42]                              |             |
|           |          | 2021 | AAVPHP.eB | CAG           | ARSA      |        | Mouse  | $5 \times 10^{11}$ vg                     | Intravenous                  | [43]                              |             |
|           |          | 2021 | AAV9      | CAG           | ARSA      |        | Mouse  | $4.0 \times 10^{11}$ vg                   | Intrathecal                  | [44]                              |             |
|           |          | 2015 | AAVrh10   | Not described | ARSA      |        | NHPs   | $1.1 \times 10^{11}$ vg total             | Brain                        | [45]                              |             |
|           |          | 2021 | AAVrh10   | Not described | ARSA      |        | NHPs   | 0.0285 or $1.5 \times 10^{12}$ gc         | Brain                        | [27]                              |             |
|           |          | 2001 | LV        | CMV           | ARSA      |        | WPRE   | Mouse                                     | 80–200 ng p24 equivalent     | Brain                             | [46]        |
|           |          | 2005 | LV        | CMV           | ARSA      |        | WPRE   | Mouse                                     | 80 ng p24 equivalent         | Brain                             | [47]        |
|           |          | 2006 | LV        | hPGK          | ARSA      |        | WPRE   | Mouse                                     | MOI = 100; $10^6$ cells      | Intravenous                       | [4]         |
|           |          | 2007 | LV        | PGK           | ARSA      |        | WPRE   | Human HSPC                                | MOI = 100                    | Intravenous                       | [48]        |
|           |          | 2010 | LV        | PGK           | ARSA      |        | WPRE   | Mouse                                     | $2 \times 10^6$ total unit   | Brain                             | [49]        |
|           |          | 2014 | LV        | EF1           | ARSA      |        | WPRE   | Mouse                                     | $2.5 \times 10^7$ total unit | Brain                             | [50]        |
|           |          | ARSB | MPS VI    | 2013          | LV        | hPGK   | ARSA   | WPREmut6                                  | Human                        | MOI = 100; $2-10 \times 10^6$ /mL | Intravenous |
| 2014      | AAV2/8   |      |           | TBG           | ARSB      |        | Mouse  | $2 \times 10^{12}$ gc/kg                  | Intravenous                  | [51]                              |             |
| 2016      | AAV2/8   |      |           | TBG           | ARSB      |        | Mouse  | $2-6 \times 10^{11}$ gc/kg                | Intravenous                  | [52]                              |             |
| 2017      | AAV2/8   |      |           | TBG           | ARSB      |        | Mouse  | $2 \times 10^{11}-2 \times 10^{12}$ gc/kg | Intravenous                  | [53]                              |             |
| 2020      | AAV2/8   |      |           | TBG           | ARSB      |        | Mouse  | 0.2 or $2 \times 10^{13}$ gc/kg           | Intravenous                  | [54]                              |             |
| 2008      | AAV2/8   |      |           | TBG           | ARSB      |        | Rat    | $4.1 \times 10^{13}$ gc/kg                | Intravenous                  | [55]                              |             |
| 2008      | AAV2/1   |      |           | CMV           | ARSB      |        | Rat    | $3.6 \times 10^{13}$ gc/kg                | Intramuscular                | [55]                              |             |
| 2002      | AAV2     |      |           | CAG           | ARSB      |        | Cat    | $0.56-1.1 \times 10^9$ particles          | Intraocular                  | [56]                              |             |
| 2008      | AAV2/8   |      |           | TBG           | ARSB      |        | Cat    | $6.6 \times 10^{13}$ gc/kg                | Intravenous                  | [55]                              |             |
| 2008      | AAV2/1   |      |           | CMV           | ARSB      |        | Cat    | $4.3 \times 10^{12}$ gc/kg                | Intramuscular                | [55]                              |             |
| 2011      | AAV2/8   |      |           | TBG           | ARSB      |        | Cat    | $0.2-6 \times 10^{13}$ gc/kg              | Intravenous                  | [57]                              |             |
| 2013      | AAV2/8   |      |           | TBG           | ARSB      |        | Cat    | $0.22 \times 10^{12}$ gc/kg               | Intravenous                  | [58]                              |             |
| 2020      | AAV2/8   |      |           | TBG           | ARSB      |        | Cat    | $2 \times 10^{12}$ gc/kg                  | Intravenous                  | [54]                              |             |



Table 3. Cont.

| Sulfatase | Disorder | Year   | Vector      | Promoter | Transgene                   | 3'-UTR                                       | Animal      | Dose                             | Route              | Ref  |
|-----------|----------|--------|-------------|----------|-----------------------------|--|-------------|----------------------------------|--------------------|------|
| GALNS     | MPS IVA  | 2020   | AAV8        | TBG      | <i>GALNS</i>                | RBG  | Mouse       | $5 \times 10^{13}$ gc/kg         | Intravenous        | [59] |
|           |          | 2020   | AAV8        | TBG      | <i>D8-GALNS</i>             | RBG  | Mouse       | $5 \times 10^{13}$ gc/kg         | Intravenous        | [59] |
|           |          | 2021   | AAV9        | CAG      | <i>GALNS</i>                |  | Rat         | $6.67 \times 10^{13}$ vg/kg      | Intravenous        | [60] |
| GNS       | MPS IID  | 2017   | AAV9        | CAG      | <i>GNS</i>                  |  | Mouse       | $5 \times 10^{10}$ vg            | Cisterna magna     | [9]  |
| SGSH      | MPS IIIA | 2007   | AAV2/5      | CMV      | <i>SGSH-IRES-SUMF1</i>      |  | Mouse       | $0.6-3 \times 10^{10}$ particles | Brain              | [61] |
|           |          | 2019   | AAV9        | CMV      | <i>IDS(1-33)-SGSH-SUMF1</i> |  | Mouse       | $5.4 \times 10^{12}$ gc/kg       | Cisterna magna     | [62] |
|           |          | 2015   | scAAVrh74   | U1a      | <i>hSGSH</i>                |  | Mouse       | $5 \times 10^{12}$ gc/kg         | Intravenous        | [63] |
|           |          | 2016   | scAAV9      | U1a      | <i>hSGSH</i>                |  | Mouse       | $1-5 \times 10^{12}$ gc/kg       | Intravenous        | [64] |
|           |          | 2016   | AAVrh10     | PGK      | <i>SGSH-IRES-SUMF1</i>      |  | Mouse       | $7.5 \times 10^9$ gc             | Brain              | [10] |
|           |          | 2018   | AAV4        | CMV      | <i>SGSH</i>                 |  | Mouse       | $5 \times 10^{10}$ particles     | Lateral ventricles | [65] |
|           |          | 2018   | AAV4        | CMV      | <i>SGSHv4</i>               |  | Mouse       | $5 \times 10^{10}$ particles     | Lateral ventricles | [65] |
|           |          | 2019   | AAVrh10     | CAG      | <i>SGSH</i>                 |  | Mouse       | $0.086-9.0 \times 10^{10}$ vg    | Brain              | [66] |
|           |          | 2019   | AAVrh10     | PGK      | <i>SGSH-IRES-SUMF1</i>      |  | Mouse       | $4.1 \times 10^9$ particles      | Brain              | [35] |
|           |          | 2019   | AAVrh10     | PGK      | <i>SGSH</i>                 |  | Mouse       | $4.1 \times 10^9$ particles      | Brain              | [35] |
|           |          | 2019   | AAVrh10     | CAG      | <i>SGSH</i>                 |  | Mouse       | $4.1 \times 10^9$ particles      | Brain              | [35] |
|           |          | 2020   | scAAV9      | mCMV     | <i>SGSH</i>                 |  | Mouse       | $0.25-5 \times 10^{13}$ vg/kg    | Intravenous        | [67] |
|           |          | 2021   | scAAV9      | U1A      | <i>SGSH</i>                 |  | Mouse       | $3 \times 10^{13}$ vg/kg         | Intravenous        | [68] |
|           |          | 2019   | AAVrh10     | CAG      | <i>SGSH</i>                 |  | NHP         | $7.2 \times 10^{11}$ vg          | Brain              | [66] |
|           |          | 2019   | AAVrh10     | CAG      | <i>SGSH</i>                 |  | Dog         | $1-2 \times 10^{12}$ vg          | Brain              | [66] |
|           |          | 2019   | AAV9        | CMV      | <i>IDS(1-33)-SGSH-SUMF1</i> |  | Pig         | $4.5 \times 10^{12}$ gc/kg       | Cisterna magna     | [62] |
|           |          | 2014   | AAVrh.10    | PGK      | <i>SGSH-IRES-SUMF1</i>      |  | Human       | $7.2 \times 10^{11}$ vg          | Brain              | [69] |
| 2012      | LV       | SFFV   | <i>SGSH</i> |          | Mouse                       | $1.5-2.5 \times 10^5$ Lin <sup>-</sup> cells | Intravenous | [70]                             |                    |      |
| 2013      | LV       | hCD11b | <i>SGSH</i> |          | Mouse                       | MOI = 30; $0.2-1 \times 10^5$ cells          | Intravenous | [71]                             |                    |      |
| 2013      | LV       | hPGK   | <i>SGSH</i> |          | Mouse                       | MOI = 30; $0.2-1 \times 10^5$ cells          | Intravenous | [71]                             |                    |      |
| 2014      | LV       | EF1a   | <i>SGSH</i> |          | Mouse                       | Not described                                | Brain       | [72]                             |                    |      |

Table 3. Cont.

| Sulfatase | Disorder | Year           | Vector               | Promoter      | Transgene                | 3'-UTR                                | Animal      | Dose   | Route   | Ref  |
|-----------|----------|----------------|----------------------|---------------|--------------------------|---------------------------------------|-------------|--|---|------|
| IDS       | MPS II   | 2014           | LV                   | EF1a          | <i>SGSH-SUMF1</i>        |                                       | Mouse       | Not described                                    | Brain   | [72] |
|           |          | 2019           | LV                   | CD11b         | <i>SGSH</i>              |                                       | Mouse       | MOI = 60; $3 \times 10^5$ Lin <sup>-</sup> cells | Intravenous   | [73] |
|           |          | 2010           | canine Ad serotype 2 | CMV           | <i>SGSH-IRES-GFP</i>     | PolyA                                 | Mouse       | $6 \times 10^9$ particles                        | Brain   | [74] |
|           |          | 2012           | canine Ad            | RSV           | <i>SGSH-IRES-GFP</i>     |                                       | Mouse       | $2 \times 10^9$ particles                        | Brain   | [75] |
|           |          | 2006           | AAV2/8               | TBG           | <i>IDS</i>               |                                       | Mouse       | $1 \times 10^{11}$ particles                     | Intravenous   | [76] |
|           |          | 2009           | AAV2/5               | CMV           | <i>IDS</i>               |                                       | Mouse       | $1 \times 10^{11}$ particles                     | Intravenous   | [77] |
|           |          | 2010           | AAV2/8               | EF            | <i>IDS</i>               | WPRES                                 | Mouse       | $1 \times 10^{11}$ particles                     | Intravenous   | [78] |
|           |          | 2016           | AAV9                 | CB            | <i>IDS</i>               | RBG                                   | Mouse       | $3 \times 10^8$ – $3 \times 10^{10}$ gc          | Intracerebroventricular                                     | [79] |
|           |          | 2016           | AAV9                 | CAG           | <i>IDS</i>               |                                       | Mouse       | $5 \times 10^{10}$ vg                            | Intracisternal<br>Intrathecal or<br>Intracerebroventricular | [80] |
|           |          | 2017           | AAV9                 | CB7           | <i>IDS</i>               | RBG                                   | Mouse       | $5.6 \times 10^{10}$ vc                          | Intravenous   | [81] |
|           |          | 2017           | AAV9                 | CB7           | <i>IDS</i>               | RBG                                   | Mouse       | $5.6 \times 10^{10}$ vc                          | Intravenous   | [81] |
|           |          | 2017           | AAV9                 | CB7           | <i>IDS-SUMF1</i>         | RBG                                   | Mouse       | $5.6 \times 10^{10}$ vc                          | Intrathecal   | [81] |
|           |          | 2017           | AAV9                 | CB7           | <i>IDS-SUMF1</i>         | RBG                                   | Mouse       | $5.6 \times 10^{10}$ vc                          | Intravenous   | [81] |
|           |          | 2017           | AAV9                 | CB7           | <i>IDS-SUMF1</i>         | RBG                                   | Mouse       |  | Intracerebroventricular                                     | [81] |
|           |          | 2018           | scAAV9               | Mini-CMV      | <i>IDS</i>               |                                       | Mouse       | $0.25$ – $2 \times 10^{13}$ vg/kg                | Intravenous   | [82] |
|           |          | 2018           | AAV2/8               | ApoE-hAAT     | <i>ZFNs + hIDS donor</i> | PolyA                                 | Mouse       | $0.25$ – $1.5 \times 10^{12}$ vg                 | Intravenous   | [83] |
|           |          | 2018           | AAV9                 | Not described | <i>IDS</i>               |                                       | NHP         | $1.7$ – $5.0 \times 10^{13}$ gc                  | Cisterna Magna  | [84] |
|           |          | 2018           | AAV9                 | Not described | <i>IDS</i>               |                                       | NHP         | $1.7$ – $5.0 \times 10^{13}$ gc                  | Suboccipital puncture                                       | [84] |
|           |          | 2015           | LV                   | MCU3          | <i>IDS</i>               |                                       | Mouse       | MOI = 50; $2 \times 10^6$ Lin <sup>-</sup> cells | Intravenous   | [85] |
|           |          | 2018           | LV                   | hCD11b        | <i>IDS</i>               | WPRES                                 | Mouse       | MOI = 100; $3$ – $4 \times 10^5$ HSCs            | Intravenous   | [86] |
| 2018      | LV       | hCD11b         | <i>IDS-ApoEII</i>    | WPRES         | Mouse                    | MOI = 100; $3$ – $4 \times 10^5$ HSCs | Intravenous | [86]   |   |      |
| 2020      | LV       | MCU3           | <i>IDS</i>           |               | Mouse                    | $1.25 \times 10^6$ cells              | Intravenous | [87]   |   |      |
| 2020      | LV       | MCU3           | <i>IDS</i>           |               | Mouse                    | $6.6$ – $7.5 \times 10^5$ cells       | Intravenous | [88]   |   |      |
| 2019      | LNP      | Not applicable | <i>IDS</i>           |               | Mouse                    | $1.5 \times 10^{12}$ vg               | Intravenous | [89]   |   |      |

AAT, human alpha 1-antitrypsin; Ad, adenovirus; BGH, bovine growth hormone polyA; CB, chicken  $\beta$ -actin promoter plus CMV enhancer; gc, genome copy; NHP, non-human primate; RBG, rabbit  $\beta$ -globin, polyA; vg, vector genome.

#### 5.4. *SGSH*

*SGSH* is an enzyme responsible for MPS type IIIA (MPS IIIA: OMIM 252900). Among the four disease subtypes of MPS III, this is the most frequently observed. MPS IIIA patients are principally found in Europe, particularly the Netherlands, but there are many patients globally [92]. For MPS IIIA, both AAV and LV gene therapies have been developed. As MPS IIIA exhibits a severe CNS phenotype but not skeletal symptoms, the delivery protocol of the transgene into the brain has been extensively studied. In the majority of animal studies, the site of AAV injection was examined to optimize the therapeutic outcomes (Table 3). In contrast, *ex vivo* transduction was selected for the LV treatment.

Similar to *ARSA*, the role of *FGE* has also been investigated in *SGSH* gene transduction [35]. First, the expression of *SUMF1* led to an enhanced *SGSH* enzymatic activity in several *in vitro* experiments. This was also true for *in vivo* experiments where the *SGSH* enzyme activity was measured in the brain. In this experiment, the *SGSH* enzymatic activity in the brain was studied with or without the *SUMF1* enzyme under the PGK promoter or the CAG promoter. Under the PGK promoter, the co-expression of this modifier enhanced *SGSH* enzymatic activity, while under the CAG promoter, the effect on the *SGSH* enzyme activity was drastic. Based on these data, a therapeutic vector with a CAG promoter for the *SGSH* transgene is currently being developed (NCT03612869).

To enhance the expression of the *SGSH* enzyme, the effect of the signal peptide *IDS* (1-33) was studied since it induces a strong secretion of proteins into the extracellular space [62]. In this case, the anticipated results were obtained.

#### 5.5. *IDS*

*IDS* is an enzyme responsible for MPS II (OMIM 309900). Its major phenotype involves CNS, skeletal deformity, and visceral manifestations. About 70% of the patients have the severe type of MPS II, presenting CNS-related symptoms [93] and a mutation of recombination or large deletion of the *IDS* gene because of the pseudogene *IDS2* located on the telomeric side of chromosome X. The remaining 30% suffer from the attenuated type of MPS II, which does not affect the CNS. Both AAV and LV gene therapies have been investigated in MPS II murine models. Similar to *MLD*, in MPS IIIA, the visceral manifestations are controlled under the existing intervention protocols. Although CNS manifestations are challenging, recent data showed that enhanced *IDS* enzymatic activity improves the brain-specific symptoms [80,82]. Similarly, a beneficial effect of LV therapy for bone manifestations has been documented [88], indicating that increased expression of the transducing gene contributes to a better therapeutic outcome.

An AAV gene therapy product is in clinical trials by REGENEXBIO Inc., (Rockville, MD, USA). This is to be injected into the brain, aiming to improve the pathology (NCT04571970). The reported animal study showed promising results; thus, similar outcomes might be obtained with the clinical study.

Moreover, Sangamo Therapeutics, Inc. provides a unique product using zinc finger technology [94]. Briefly, they use three AAV vectors for gene editing. The first two vectors express two zinc fingers targeting the albumin locus of the hepatocyte. The third vector expresses the donor sequence of the transgene. Under optimal conditions where all three vectors are expressed in a single cell in the liver, expression of the *IDS* gene under the endogenous albumin promoter is expected [83]. Currently, a clinical trial is ongoing (NCT03041324).

## 6. Emerging Techniques

### 6.1. Lipid Nanoparticle (LNP)

LNP is a non-viral delivery method for mRNA-based medicine [95]. The history of LNP research originates in the study of liposomes, but this innovative technology that is directly applicable to gene therapy has advanced in recent years. Still, there are several areas for improvement. First, the lipid used for LNP is carefully examined. Based on synthetic chemistry, synthetic lipids, collectively called cation-ionizable lipids, show great

potential for gene delivery *in vivo* because of their long life, low toxicity, and the potential for the modification of the LNP surface by antibodies, leading to the production of a sophisticated drug delivery system of transgenes with specific tropisms [96].

The development of this technology began before the mRNA vaccine against COVID-19, the pandemic that emerged in late 2019. Another reason for the ease of *in vivo* use of this technology is the advances in stabilization technology for mRNA. Generally, mRNA is thought to be more fragile than DNA due to the presence of RNases in the laboratory setting. However, recent advances in the improvement of mRNA stability solved several of these issues. One issue of mRNA instability relates to its 5'-cap structure. A new technology that replaces the wild-type ribonucleic acid with a 2'-O-methoxy analog enhances mRNA stability. Moreover, this replacement makes the product resistant to degradation by RNases. For example, pseudouridine is a uridine analog found at a proportion of approximately 5% compared to uridine. Due to the impaired susceptibility of pseudouridine-containing mRNA to RNase, this modified mRNA has been used for the synthesis of RNA with a prolonged half-life *in vivo*. Additionally, the length of poly-A affects the cellular half-life of mRNA. The optimization of these multiple parameters *in silico* can convert the prototypical mRNA delivery agent into a valuable final product.

### 6.2. Gene Delivery

For safety reasons, intravenous administration has often been chosen for gene delivery. In LSD treatment, the brain is a key target. In this case, the direct injection of agents into the brain is needed. To administer a relatively large amount of agents across an entire brain area, intrathecal, intracisternal, and intracerebroventricular administration have been used [97] (Table 3). Apart from these delivery techniques, the intranasal administration of drugs has also been investigated. After intranasal administration, the enzymatic activity in the olfactory bulb recovered to 100-fold compared to the control, maintaining the same levels in the rest of the brain [98]. Recent studies reported the efficacy of the *in utero* administration of viral vectors in the mouse, demonstrating promising outcomes [99,100].

### 6.3. Peptide Modifiers

In the last decades, efforts to screen peptides that enhance the penetration of drugs through the blood–brain barrier have been made, reporting numerous such peptides [101]. The relevant sequences of these peptides are found in the part of the endogenous protein that penetrates the blood–brain barrier either by itself or by a receptor–ligand mechanism. Zhang et al. [102] recently reported that the dodecapeptide PB5-3 enhances the transduction of AAV9 to the brain. The sequence of this peptide has no similarity to known sequences of proteins/peptides, with approximately 2- to 3-fold increases in AAV9 transduction in the brain compared to intravenous administration. The detailed mechanism of this effect remains to be elucidated. Furthermore, the combination of the AAV serotype and the peptide sequence plays an essential role in determining the efficacy of the peptide modifiers.

### 6.4. CRISPR/Cas9

The genetic correction of pathogenic genes is becoming an essential technology in research and medicine. A recent study reported a CRISPR/Cas9 correction of the *ARSA* gene *in vitro* [103]. In this experiment, patient-derived hematopoietic stem/progenitor cells were treated with five guide RNAs (gRNAs) at the 5'-UTR or in close proximity to the transcription start site of the *ARSA* gene, which allowed the recombination of codon-optimized therapeutic *ARSA* cDNA using AAV6. The optimization of the experimental setting included (i) gRNA sequences, (ii) multiplicity of infection, and (iii) the molar ratio of the ribonuclease protein consisting of Cas9 protein and gRNA. The authors reported that 16.6–37% of the GFP<sup>+</sup> transduced cells were detected by FACS analysis, and a 19- to 32-fold increase in *ARSA* activity was documented with an enzyme assay. The advantages of this technique include the following: (i) a single set of pre-examined gRNAs that cleaves at the 5'-UTR or in close proximity to the transcription start site of the gene of interest can be used

for many pathogenic genes; (ii) due to the insertion at a known locus by CRISPR/Cas9, there is no possibility of random integration when LV is used; (iii) the use of a codon-optimized therapeutic cDNA allows for maximal enzyme expression; and (iv) the use of an exogenous gene (e.g., the SV40 poly-A region) in the repair template prevents a second cleavage after the recombination. A similar technique has been used in immunodeficiency (SCID-X1), Wiskott–Aldrich syndrome, and severe congenital neutropenia [104–106]. However, this novel protocol for the ARSA gene uses lower amounts of the vector at only two orders of magnitude.

## 7. Future Perspectives

A growing number of gene therapy products have recently been developed. Both AAV and LV are established vehicles of gene therapy. A known disadvantage of AAV is the amount of the therapeutic vector required for effective treatment. Innovations to reduce this burden, such as the threonine-to-phenylalanine replacement described by Zhong et al. [26], may help improve this situation. Moreover, the production of antibodies against the capsid protein of AAV is confounding. For LV, the application is largely limited to hematopoietic stem cell transplantation. However, these are relatively minor issues compared to the fact that no known severe adverse events have been reported for these vectors. Further research on emerging techniques may help improve the vectors' safety and application.

**Author Contributions:** Conceptualization, M.N. and R.M.; writing—original draft preparation, review and editing, R.M. All authors have read and agreed to the published version of the manuscript.

**Funding:** This work was supported by a grant-in-aid from AMED (22ae0201004h0005) to M.N. and R.M. and a grant-in-aid from MEXT (22K07927; 19K07952) to R.M.

**Acknowledgments:** R.M. acknowledges M.N.'s scientific input.

**Conflicts of Interest:** The authors declare no conflict of interest.

## References

1. Clarke, T.; Fernandez, F.E.; Dawson, P.A. Sulfation Pathways During Neurodevelopment. *Front. Mol. Biosci.* **2022**, *9*, 866196. [[CrossRef](#)] [[PubMed](#)]
2. Barbeyron, T.; Brillet-Guéguen, L.; Carré, W.; Carrière, C.; Caron, C.; Czjzek, M.; Hoebeke, M.; Michel, G. Matching the Diversity of Sulfated Biomolecules: Creation of a Classification Database for Sulfatases Reflecting Their Substrate Specificity. *PLoS ONE* **2016**, *11*, e0164846. [[CrossRef](#)] [[PubMed](#)]
3. Hettle, A.G.; Vickers, C.J.; Boraston, A.B. Sulfatases: Critical Enzymes for Algal Polysaccharide Processing. *Front. Plant Sci.* **2022**, *13*, 837636. [[CrossRef](#)] [[PubMed](#)]
4. Biffi, A.; Capotondo, A.; Fasano, S.; del Carro, U.; Marchesini, S.; Azuma, H.; Malaguti, M.C.; Amadio, S.; Brambilla, R.; Grompe, M.; et al. Gene Therapy of Metachromatic Leukodystrophy Reverses Neurological Damage and Deficits in Mice. *J. Clin. Investig.* **2006**, *116*, 3070–3082. [[CrossRef](#)]
5. Hendrickx, G.; Danyukova, T.; Baranowsky, A.; Rolvien, T.; Angermann, A.; Schweizer, M.; Keller, J.; Schröder, J.; Meyer-Schwesinger, C.; Muschol, N.; et al. Enzyme Replacement Therapy in Mice Lacking Arylsulfatase B Targets Bone-Remodeling Cells, but not Chondrocytes. *Hum. Mol. Genet.* **2020**, *29*, 803–816. [[CrossRef](#)]
6. Kowalewski, B.; Lamanna, W.C.; Lawrence, R.; Damme, M.; Stroobants, S.; Padva, M.; Kalus, I.; Frese, M.A.; Lubke, T.; Lüllmann-Rauch, R.; et al. Arylsulfatase G Inactivation Causes Loss of Heparan Sulfate 3-O-Sulfatase Activity and Mucopolysaccharidosis in Mice. *Proc. Natl. Acad. Sci. USA* **2012**, *109*, 10310–10315. [[CrossRef](#)]
7. Trabszo, C.; Ramms, B.; Chopra, P.; Lüllmann-Rauch, R.; Stroobants, S.; Sproß, J.; Jeschke, A.; Schinke, T.; Boons, G.J.; Esko, J.D.; et al. Arylsulfatase K Inactivation Causes Mucopolysaccharidosis Due to Deficient Glucuronate Desulfation of Heparan and Chondroitin Sulfate. *Biochem. J.* **2020**, *477*, 3433–3451. [[CrossRef](#)]
8. Tomatsu, S.; Gutierrez, M.; Nishioka, T.; Yamada, M.; Yamada, M.; Tosaka, Y.; Grubb, J.H.; Montañó, A.M.; Vieira, M.B.; Trandafirescu, G.G.; et al. Development of MPS IVA Mouse (Galntm(hC79S.mC76S)slu) Tolerant to Human N-Acetylgalactosamine-6-Sulfate Sulfatase. *Hum. Mol. Genet.* **2005**, *14*, 3321–3335. [[CrossRef](#)]
9. Roca, C.; Motas, S.; Marco, S.; Ribera, A.; Sanchez, V.; Sanchez, X.; Bertolin, J.; Leon, X.; Perez, J.; Garcia, M.; et al. Disease Correction by AAV-Mediated Gene Therapy in a New Mouse Model of Mucopolysaccharidosis Type IIID. *Hum. Mol. Genet.* **2017**, *26*, 1535–1551. [[CrossRef](#)]
10. Winner, L.K.; Beard, H.; Hassiotis, S.; Lau, A.A.; Luck, A.J.; Hopwood, J.J.; Hemsley, K.M. A Preclinical Study Evaluating AAVrh10-Based Gene Therapy for Sanfilippo Syndrome. *Hum. Gene Ther.* **2016**, *27*, 363–375. [[CrossRef](#)]

11. Garcia, A.R.; Pan, J.; Lamsa, J.C.; Muenzer, J. The Characterization of a Murine Model of Mucopolysaccharidosis II (Hunter Syndrome). *J. Inher. Metab. Dis.* **2007**, *30*, 924–934. [[CrossRef](#)] [[PubMed](#)]
12. Holst, C.R.; Bou-Reslan, H.; Gore, B.B.; Wong, K.; Grant, D.; Chalasani, S.; Carano, R.A.; Frantz, G.D.; Tessier-Lavigne, M.; Bolon, B.; et al. Secreted Sulfatases Sulf1 and Sulf2 Have Overlapping Yet Essential Roles in Mouse Neonatal Survival. *PLoS ONE* **2007**, *2*, e575. [[CrossRef](#)] [[PubMed](#)]
13. Preusser-Kunze, A.; Mariappan, M.; Schmidt, B.; Gande, S.L.; Mutenda, K.; Wenzel, D.; von Figura, K.; Dierksl, T. Molecular Characterization of the Human Calpha-Formylglycine-Generating Enzyme. *J. Biol. Chem.* **2005**, *280*, 14900–14910. [[CrossRef](#)]
14. Appel, M.J.; Meier, K.K.; Lafrance-Vanasse, J.; Lim, H.; Tsai, C.L.; Hedman, B.; Hodgson, K.O.; Tainer, J.A.; Solomon, E.I.; Bertozzi, C.R. Formylglycine-Generating Enzyme Binds Substrate Directly at a Mononuclear Cu(I) Center to Initiate O<sub>2</sub> Activation. *Proc. Natl. Acad. Sci. USA* **2019**, *116*, 5370–5375. [[CrossRef](#)]
15. Dierks, T.; Schmidt, B.; Borissenko, L.V.; Peng, J.; Preusser, A.; Mariappan, M.; von Figura, K. Multiple Sulfatase Deficiency Is Caused by Mutations in the Gene Encoding the Human C(Alpha)-Formylglycine Generating Enzyme. *Cell* **2003**, *113*, 435–444. [[CrossRef](#)]
16. Muenzer, J. Overview of the Mucopolysaccharidoses. *Rheumatology* **2011**, *50*, v4–v12. [[CrossRef](#)]
17. Biffi, A.; Montini, E.; Lorioli, L.; Cesani, M.; Fumagalli, F.; Plati, T.; Baldoli, C.; Martino, S.; Calabria, A.; Canale, S.; et al. Lentiviral Hematopoietic Stem Cell Gene Therapy Benefits Metachromatic Leukodystrophy. *Science* **2013**, *341*, 1233158. [[CrossRef](#)]
18. Brunetti-Pierri, N.; Andreucci, M.V.; Tuzzi, R.; Vega, G.R.; Gray, G.; McKeown, C.; Ballabio, A.; Andria, G.; Meroni, G.; Parenti, G. X-Linked Recessive Chondrodysplasia Punctata: Spectrum of Arylsulfatase E Gene Mutations and Expanded Clinical Variability. *Am. J. Med. Genet. A* **2003**, *117A*, 164–168. [[CrossRef](#)]
19. Reed, M.J.; Purohit, A.; Woo, L.W.L.; Newman, S.P.; Potter, B.V.L. Steroid Sulfatase: Molecular Biology, Regulation, and Inhibition. *Endocr. Rev.* **2005**, *26*, 171–202. [[CrossRef](#)]
20. Baek, H.S.; Kwon, T.U.; Shin, S.; Kwon, Y.J.; Chun, Y.J. Steroid Sulfatase Deficiency Causes Cellular Senescence and Abnormal Differentiation by Inducing Yippee-Like 3 Expression in Human Keratinocytes. *Sci. Rep.* **2021**, *11*, 20867. [[CrossRef](#)]
21. Platt, F.M.; d’Azzo, A.; Davidson, B.L.; Neufeld, E.F.; Tiffit, C.J. Lysosomal Storage Diseases. *Nat. Rev. Dis. Prim.* **2018**, *4*, 27. [[CrossRef](#)] [[PubMed](#)]
22. Muenzer, J.; Vijayaraghavan, S.; Stein, M.; Kearney, S.; Wu, Y.; Alexanderian, D. Long-Term Open-Label Phase I/II Extension Study of Intrathecal Idursulfase-IT in the Treatment of Neuronopathic Mucopolysaccharidosis II. *Genet. Med.* **2022**, *24*, 1437–1448. [[CrossRef](#)] [[PubMed](#)]
23. Sonoda, H.; Morimoto, H.; Yoden, E.; Koshimura, Y.; Kinoshita, M.; Golovina, G.; Takagi, H.; Yamamoto, R.; Minami, K.; Mizoguchi, A.; et al. A Blood-Brain-Barrier-Penetrating Anti-Human Transferrin Receptor Antibody Fusion Protein for Neuronopathic Mucopolysaccharidosis II. *Mol. Ther.* **2018**, *26*, 1366–1374. [[CrossRef](#)] [[PubMed](#)]
24. Arguello, A.; Meisner, R.; Thomsen, E.R.; Nguyen, H.N.; Ravi, R.; Simms, J.; Lo, I.; Speckart, J.; Holtzman, J.; Gill, T.M.; et al. Iduronate-2-Sulfatase Transport Vehicle Rescues Behavioral and Skeletal Phenotypes in a Mouse Model of Hunter Syndrome. *JCI Insight* **2021**, *6*, e145445. [[CrossRef](#)] [[PubMed](#)]
25. Hastie, E.; Samulski, R.J. Adeno-Associated Virus at 50: A golden Anniversary of Discovery, Research, and Gene Therapy Success—A Personal Perspective. *Hum. Gene Ther.* **2015**, *26*, 257–265. [[CrossRef](#)]
26. Zhong, L.; Li, B.; Mah, C.S.; Govindasamy, L.; Agbandje-McKenna, M.; Cooper, M.; Herzog, R.W.; Zolotukhin, I.; Warrington, K.H.; Weigel-Van Aken, K.A.; et al. Next Generation of Adeno-Associated Virus 2 Vectors: Point Mutations in Tyrosines Lead to High-Efficiency Transduction at Lower Doses. *Proc. Natl. Acad. Sci. USA* **2008**, *105*, 7827–7832. [[CrossRef](#)] [[PubMed](#)]
27. Rosenberg, J.B.; Chen, A.; De, B.P.; Dyke, J.P.; Ballon, D.J.; Monette, S.; Arbona, R.J.R.; Kaminsky, S.M.; Crystal, R.G.; Sondhi, D. Safety of Direct Intraparenchymal AAVrh.10-Mediated Central Nervous System Gene Therapy for Metachromatic Leukodystrophy. *Hum. Gene Ther.* **2021**, *32*, 563–580. [[CrossRef](#)]
28. Ferrari, G.; Thrasher, A.J.; Aiuti, A. Gene Therapy Using Haematopoietic Stem and Progenitor Cells. *Nat. Rev. Genet.* **2021**, *22*, 216–234. [[CrossRef](#)]
29. Rintz, E.; Higuchi, T.; Kobayashi, H.; Galileo, D.S.; Wegrzyn, G.; Tomatsu, S. Promoter Considerations in the Design of Lentiviral Vectors for Use in Treating Lysosomal Storage Diseases. *Mol. Ther. Methods Clin. Dev.* **2021**, *24*, 71–87. [[CrossRef](#)]
30. Hong, X.; Daiker, J.; Sadilek, M.; Ruiz-Schultz, N.; Kumar, A.B.; Norcross, S.; Dansithong, W.; Suhr, T.; Escolar, M.L.; Scott, C.R.; et al. Toward Newborn Screening of Metachromatic Leukodystrophy: Results from Analysis of over 27,000 Newborn Dried Blood Spots. *Genet. Med.* **2021**, *23*, 555–561. [[CrossRef](#)]
31. Hong, X.; Kumar, A.B.; Daiker, J.; Yi, F.; Sadilek, M.; de Mattia, F.; Fumagalli, F.; Calbi, V.; Damiano, R.; della Bona, M.; et al. Leukocyte and Dried Blood Spot Arylsulfatase a Assay by Tandem Mass Spectrometry. *Anal. Chem.* **2020**, *92*, 6341–6348. [[CrossRef](#)] [[PubMed](#)]
32. Sessa, M.; Lorioli, L.; Fumagalli, F.; Acquati, S.; Redaelli, D.; Baldoli, C.; Canale, S.; Lopez, I.D.; Morena, F.; Calabria, A.; et al. Lentiviral Haemopoietic Stem-Cell Gene Therapy in Early-Onset Metachromatic Leukodystrophy: An Ad-Hoc Analysis of a Non-Randomised, Open-Label, Phase 1/2 Trial. *Lancet (Lond. Engl.)* **2016**, *388*, 476–487. [[CrossRef](#)]
33. Fumagalli, F.; Calbi, V.; Sora, M.G.N.; Sessa, M.; Baldoli, C.; Rancoita, P.M.V.; Ciotti, F.; Sarzana, M.; Frascini, M.; Zambon, A.A.; et al. Lentiviral Haematopoietic Stem-Cell Gene Therapy for Early-Onset Metachromatic Leukodystrophy: Long-Term Results from a Non-Randomised, Open-Label, Phase 1/2 Trial and Expanded Access. *Lancet* **2022**, *399*, 372–383. [[CrossRef](#)]

34. Dierks, T.; Dickmanns, A.; Preusser-Kunze, A.; Schmidt, B.; Mariappan, M.; von Figura, K.; Ficner, R.; Rudolph, M.G. Molecular Basis for Multiple Sulfatase Deficiency and Mechanism for Formylglycine Generation of the Human Formylglycine-Generating Enzyme. *Cell* **2005**, *121*, 541–552. [[CrossRef](#)] [[PubMed](#)]
35. Gray, A.L.; O’Leary, C.; Liao, A.; Agúndez, L.; Youshani, A.S.; Gleitz, H.F.; Parker, H.; Taylor, J.T.; Danos, O.; Hocquemiller, M.; et al. An Improved Adeno-Associated Virus Vector for Neurological Correction of the Mouse Model of Mucopolysaccharidosis IIIA. *Hum. Gene Ther.* **2019**, *30*, 1052–1066. [[CrossRef](#)] [[PubMed](#)]
36. Kurai, T.; Hisayasu, S.; Kitagawa, R.; Migita, M.; Suzuki, H.; Hirai, Y.; Shimada, T. AAV1 Mediated Co-Expression of Formylglycine-Generating Enzyme and Arylsulfatase a Efficiently Corrects Sulfatide Storage in a Mouse Model of Metachromatic Leukodystrophy. *Mol. Ther.* **2007**, *15*, 38–43. [[CrossRef](#)] [[PubMed](#)]
37. Sevin, C.; Benraiss, A.; van Dam, D.; Bonnin, D.; Nagels, G.; Verot, L.; Laurendeau, I.; Vidaud, M.; Gieselmann, V.; Vanier, M.; et al. Intracerebral Adeno-Associated Virus-Mediated Gene Transfer in Rapidly Progressive Forms of Metachromatic Leukodystrophy. *Hum. Mol. Genet.* **2006**, *15*, 53–64. [[CrossRef](#)]
38. Iwamoto, N.; Watanabe, A.; Yamamoto, M.; Miyake, N.; Kurai, T.; Teramoto, A.; Shimada, T. Global Diffuse Distribution in the Brain and Efficient Gene Delivery to the Dorsal Root Ganglia by Intrathecal Injection of Adeno-Associated Viral Vector Serotype 1. *J. Gene Med.* **2009**, *11*, 498–505. [[CrossRef](#)]
39. Pigué, F.; Sondhi, D.; Piraud, M.; Fouquet, F.; Hackett, N.R.; Ahouansou, O.; Vanier, M.T.; Bieche, I.; Aubourg, P.; Crystal, R.G.; et al. Correction of Brain Oligodendrocytes by AAVrh.10 Intracerebral Gene Therapy in Metachromatic Leukodystrophy Mice. *Hum. Gene Ther.* **2012**, *23*, 903–914. [[CrossRef](#)]
40. Rosenberg, J.B.; Sondhi, D.; Rubin, D.G.; Monette, S.; Chen, A.; Cram, S.; De, B.P.; Kaminsky, S.M.; Sevin, C.; Aubourg, P.; et al. Comparative Efficacy and Safety of Multiple Routes of Direct CNS Administration of Adeno-Associated Virus Gene Transfer Vector Serotype rh.10 Expressing the Human Arylsulfatase A cDNA to Nonhuman Primates. *Hum. Gene Ther. Clin. Dev.* **2014**, *25*, 164–177. [[CrossRef](#)]
41. Miyake, N.; Miyake, K.; Asakawa, N.; Yamamoto, M.; Shimada, T. Long-Term Correction of Biochemical and Neurological Abnormalities in MLD Mice Model by Neonatal Systemic Injection of an AAV Serotype 9 vector. *Gene Ther.* **2014**, *21*, 427–433. [[CrossRef](#)] [[PubMed](#)]
42. Hironaka, K.; Yamazaki, Y.; Hirai, Y.; Yamamoto, M.; Miyake, N.; Miyake, K.; Okada, T.; Morita, A.; Shimada, T. Enzyme Replacement in the CSF to Treat Metachromatic Leukodystrophy in Mouse Model Using Single Intracerebroventricular Injection of Self-Complementary AAV1 Vector. *Sci. Rep.* **2015**, *5*, 13104. [[CrossRef](#)] [[PubMed](#)]
43. Audouard, E.; Oger, V.; Meha, B.; Cartier, N.; Sevin, C.; Pigué, F. Complete Correction of Brain and Spinal Cord Pathology in Metachromatic Leukodystrophy Mice. *Front. Mol. Neurosci.* **2021**, *14*, 677895. [[CrossRef](#)] [[PubMed](#)]
44. Miyake, N.; Miyake, K.; Sakai, A.; Yamamoto, M.; Suzuki, H.; Shimada, T. Treatment of Adult Metachromatic Leukodystrophy Model Mice Using Intrathecal Administration of Type 9 AAV Vector Encoding Arylsulfatase A. *Sci. Rep.* **2021**, *11*, 20513. [[CrossRef](#)]
45. Zerah, M.; Pigué, F.; Colle, M.A.; Raoul, S.; Deschamps, J.Y.; Deniaud, J.; Gautier, B.; Toulgoat, F.; Bieche, I.; Laurendeau, I.; et al. Intracerebral Gene Therapy Using AAVrh.10-hARSA Recombinant Vector to Treat Patients with Early-Onset Forms of Metachromatic Leukodystrophy: Preclinical Feasibility and Safety Assessments in Nonhuman Primates. *Hum. Gene Ther. Clin. Dev.* **2015**, *26*, 113–124. [[CrossRef](#)]
46. Consiglio, A.; Quattrini, A.; Martino, S.; Bensadoun, J.C.; Dolcetta, D.; Trojani, A.; Benaglia, G.; Marchesini, S.; Cestari, V.; Oliverio, A.; et al. In Vivo Gene Therapy Of Metachromatic Leukodystrophy by Lentiviral Vectors: Correction of Neuropathology and Protection Against Learning Impairments in Affected Mice. *Nat. Med.* **2001**, *7*, 310–316. [[CrossRef](#)]
47. Luca, T.; Givogri, M.I.; Perani, L.; Galbiati, F.; Follenzi, A.; Naldini, L.; Bongarzone, E.R. Axons Mediate the Distribution of Arylsulfatase a Within the Mouse Hippocampus Upon Gene Delivery. *Mol. Ther.* **2005**, *12*, 669–679. [[CrossRef](#)]
48. Capotondo, A.; Cesani, M.; Pepe, S.; Fasano, S.; Gregori, S.; Tononi, L.; Venneri, M.A.; Brambilla, R.; Quattrini, A.; Ballabio, A.; et al. Safety of arylsulfatase A Overexpression for Gene Therapy of Metachromatic Leukodystrophy. *Hum. Gene Ther.* **2007**, *18*, 821–836. [[CrossRef](#)]
49. Lattanzi, A.; Neri, M.; Maderna, C.; di Girolamo, I.; Martino, S.; Orlacchio, A.; Amendola, M.; Naldini, L.; Gritti, A. Widespread Enzymatic Correction of CNS Tissues by a Single Intracerebral Injection of Therapeutic Lentiviral Vector in Leukodystrophy Mouse Models. *Hum. Mol. Genet.* **2010**, *19*, 2208–2227. [[CrossRef](#)]
50. McAllister, R.G.; Liu, J.; Woods, M.W.; Tom, S.K.; Rupa, A.; Barr, S.D. Lentivector Integration Sites in Ependymal Cells from a Model of Metachromatic Leukodystrophy: Non-B DNA as a New Factor Influencing Integration. *Mol. Ther. Nucleic Acids* **2014**, *3*, e187. [[CrossRef](#)]
51. Ferla, R.; Claudiani, P.; Cotugno, G.; Saccone, P.; de Leonibus, E.; Auricchio, A. Similar Therapeutic Efficacy between a single Administration of Gene Therapy and Multiple Administrations of Recombinant Enzyme in a Mouse Model of Lysosomal Storage Disease. *Hum. Gene Ther.* **2014**, *25*, 609–618. [[CrossRef](#)] [[PubMed](#)]
52. Alliegro, M.; Ferla, R.; Nusco, E.; de Leonibus, C.; Settembre, C.; Auricchio, A. Low-Dose Gene Therapy Reduces the Frequency of Enzyme Replacement Therapy in a Mouse Model of Lysosomal Storage Disease. *Mol. Ther.* **2016**, *24*, 2054–2063. [[CrossRef](#)] [[PubMed](#)]

53. Ferla, R.; Alliegro, M.; Marteau, J.B.; Dell'Anno, M.; Nusco, E.; Pouillot, S.; Galimberti, S.; Valsecchi, M.G.; Zuliani, V.; Auricchio, A. Non-Clinical Safety and Efficacy of an AAV2/8 Vector Administered Intravenously for Treatment of Mucopolysaccharidosis Type VI. *Mol. Ther. Methods Clin. Dev.* **2017**, *6*, 143–158. [[CrossRef](#)] [[PubMed](#)]
54. Ferla, R.; Alliegro, M.; Dell'Anno, M.; Nusco, E.; Cullen, J.M.; Smith, S.N.; Wolfsberg, T.G.; O'Donnell, P.; Wang, P.; Nguyen, A.D.; et al. Low Incidence of Hepatocellular Carcinoma in Mice and Cats Treated with Systemic Adeno-Associated Viral Vectors. *Mol. Ther. Methods Clin. Dev.* **2020**, *20*, 247–257. [[CrossRef](#)]
55. Tessitore, A.; Faella, A.; O'Malley, T.; Cotugno, G.; Doria, M.; Kunieda, T.; Matarese, G.; Haskins, M.; Auricchio, A. Biochemical, Pathological, and Skeletal Improvement of Mucopolysaccharidosis VI after Gene Transfer to Liver but not to Muscle. *Mol. Ther.* **2008**, *16*, 30–37. [[CrossRef](#)]
56. Ho, T.T.; Maguire, A.M.; Aguirre, G.D.; Surace, E.M.; Anand, V.; Zeng, Y.; Salvetti, A.; Hopwood, J.J.; Haskins, M.E.; Bennett, J. Phenotypic Rescue after Adeno-Associated Virus-Mediated Delivery of 4-Sulfatase to the Retinal Pigment Epithelium of Feline Mucopolysaccharidosis VI. *J. Gene Med.* **2002**, *4*, 613–621. [[CrossRef](#)]
57. Cotugno, G.; Annunziata, P.; Tessitore, A.; O'Malley, T.; Capalbo, A.; Faella, A.; Bartolomeo, R.; O'Donnell, P.; Wang, P.; Russo, F.; et al. Long-Term Amelioration of feline Mucopolysaccharidosis VI after AAV-Mediated Liver Gene Transfer. *Mol. Ther.* **2011**, *19*, 461–469. [[CrossRef](#)]
58. Ferla, R.; O'Malley, T.; Calcedo, R.; O'Donnell, P.; Wang, P.; Cotugno, G.; Claudiani, P.; Wilson, J.M.; Haskins, M.; Auricchio, A. Gene Therapy for Mucopolysaccharidosis Type VI is Effective in Cats Without Pre-Existing Immunity to AAV8. *Hum. Gene Ther.* **2013**, *24*, 163–169. [[CrossRef](#)]
59. Sawamoto, K.; Karumuthil-Melethil, S.; Khan, S.; Stapleton, M.; Bruder, J.T.; Danos, O.; Tomatsu, S. Liver-Targeted AAV8 Gene Therapy Ameliorates Skeletal and Cardiovascular Pathology in a Mucopolysaccharidosis IVA Murine Model. *Mol. Ther. Methods Clin. Dev.* **2020**, *18*, 50–61. [[CrossRef](#)]
60. Bertolin, J.; Sánchez, V.; Ribera, A.; Jaén, M.L.; Garcia, M.; Pujol, A.; Sánchez, X.; Muñoz, S.; Marcó, S.; Pérez, J.; et al. Treatment of Skeletal and Non-Skeletal Alterations of Mucopolysaccharidosis Type IVA by AAV-Mediated Gene Therapy. *Nat. Commun.* **2021**, *12*, 5343. [[CrossRef](#)]
61. Fraldi, A.; Hemsley, K.; Crawley, A.; Lombardi, A.; Lau, A.; Sutherland, L.; Auricchio, A.; Ballabio, A.; Hopwood, J.J. Functional Correction of CNS Lesions in an MPS-IIIa Mouse Model by Intracerebral AAV-Mediated Delivery of Sulfamidase and SUMF1 Genes. *Hum. Mol. Genet.* **2007**, *16*, 2693–2702. [[CrossRef](#)] [[PubMed](#)]
62. Sorrentino, N.C.; Cacace, V.; de Risi, M.; Maffia, V.; Strollo, S.; Tedesco, N.; Nusco, E.; Romagnoli, N.; Ventrella, D.; Huang, Y.; et al. Enhancing the Therapeutic Potential of Sulfamidase for the Treatment of Mucopolysaccharidosis IIIa. *Mol. Ther. Methods Clin. Dev.* **2019**, *15*, 333–342. [[CrossRef](#)] [[PubMed](#)]
63. Duncan, F.J.; Naughton, B.J.; Zaraspe, K.; Murrey, D.A.; Meadows, A.S.; Clark, K.R.; Newsom, D.E.; White, P.; Fu, H.; McCarty, D.M. Broad Functional Correction of Molecular Impairments by Systemic Delivery of scAAVrh74-hSGSH Gene Delivery in MPS IIIa Mice. *Mol. Ther.* **2015**, *23*, 638–647. [[CrossRef](#)] [[PubMed](#)]
64. Fu, H.; Cataldi, M.P.; Ware, T.A.; Zaraspe, K.; Meadows, A.S.; Murrey, D.A.; McCarty, D.M. Functional Correction of Neurological and Somatic Disorders at Later Stages of Disease in MPS IIIa Mice by Systemic scAAV9-hSGSH Gene Delivery. *Mol. Ther. Methods Clin. Dev.* **2016**, *3*, 16036. [[CrossRef](#)]
65. Chen, Y.; Zheng, S.; Tecedor, L.; Davidson, B.L. Overcoming Limitations Inherent in Sulfamidase to Improve Mucopolysaccharidosis IIIa Gene Therapy. *Mol. Ther.* **2018**, *26*, 1118–1126. [[CrossRef](#)] [[PubMed](#)]
66. Hocquemiller, M.; Hemsley, K.M.; Douglass, M.L.; Tamang, S.J.; Neumann, D.; King, B.M.; Beard, H.; Trim, P.J.; Winner, L.K.; Lau, A.A.; et al. AAVrh10 Vector Corrects Disease Pathology in MPS IIIa Mice and Achieves Widespread Distribution of SGSH in Large Animal Brains. *Mol. Ther. Methods Clin. Dev.* **2019**, *17*, 174–187. [[CrossRef](#)]
67. Bobo, T.A.; Samowitz, P.N.; Robinson, M.I.; Fu, H. Targeting the Root Cause of Mucopolysaccharidosis IIIa with a New scAAV9 Gene Replacement Vector. *Mol. Ther. Methods Clin. Dev.* **2020**, *19*, 474–485. [[CrossRef](#)]
68. Saville, J.T.; Derrick-Roberts, A.L.K.; Mcintyre, C.; Fuller, M. Systemic scAAV9.U1a.hSGSH Delivery Corrects Brain Biochemistry in Mucopolysaccharidosis Type IIIa at Early and Later Stages of Disease. *Hum. Gene Ther.* **2021**, *32*, 420–430. [[CrossRef](#)]
69. Tardieu, M.; Zérah, M.; Husson, B.; de Bournonville, S.; Deiva, K.; Adamsbaum, C.; Vincent, F.; Hocquemiller, M.; Broissand, C.; Furlan, V.; et al. Intracerebral Administration of Adeno-Associated Viral Vector Serotype rh.10 Carrying Human SGSH and SUMF1 cDNAs in Children With Mucopolysaccharidosis Type IIIa Disease: Results of a Phase I/II Trial. *Hum. Gene Ther.* **2014**, *25*, 506–516. [[CrossRef](#)]
70. Langford-Smith, A.; Wilkinson, F.L.; Langford-Smith, K.J.; Holley, R.J.; Sergijenko, A.; Howe, S.J.; Bennett, W.R.; Jones, S.A.; Wraith, J.E.; Merry, C.L.R.; et al. Hematopoietic Stem Cell and Gene Therapy Corrects Primary Neuropathology and Behavior in Mucopolysaccharidosis IIIa Mice. *Mol. Ther.* **2012**, *20*, 1610–1621. [[CrossRef](#)]
71. Sergijenko, A.; Langford-Smith, A.; Liao, A.Y.; Pickford, C.E.; McDermott, J.; Nowinski, G.; Langford-Smith, K.J.; Merry, C.L.; Jones, S.A.; Wraith, J.E.; et al. Myeloid/Microglial Driven Autologous Hematopoietic Stem Cell Gene Therapy Corrects a Neuronopathic Lysosomal Disease. *Mol. Ther.* **2013**, *21*, 1938–1949. [[CrossRef](#)] [[PubMed](#)]
72. Mcintyre, C.; Derrick-Roberts, A.L.K.; Byers, S.; Anson, D.S. Correction of Murine Mucopolysaccharidosis Type IIIa Central Nervous System Pathology by Intracerebroventricular Lentiviral-Mediated Gene Delivery. *J. Gene Med.* **2014**, *16*, 374–387. [[CrossRef](#)] [[PubMed](#)]



73. Ellison, S.M.; Liao, A.; Wood, S.; Taylor, J.; Youshani, A.S.; Rowston, S.; Parker, H.; Armant, M.; Biffi, A.; Chan, L.; et al. Pre-clinical Safety and Efficacy of Lentiviral Vector-Mediated Ex Vivo Stem Cell Gene Therapy for the Treatment of Mucopolysaccharidosis IIIA. *Mol. Ther. Methods Clin. Dev.* **2019**, *13*, 399–413. [[CrossRef](#)]
74. Lau, A.A.; Hopwood, J.J.; Kremer, E.J.; Hemsley, K.M. SGSH Gene Transfer in Mucopolysaccharidosis Type IIIA Mice Using Canine Adenovirus Vectors. *Mol. Genet. Metab.* **2010**, *100*, 168–175. [[CrossRef](#)] [[PubMed](#)]
75. Lau, A.A.; Rozaklis, T.; Ibanes, S.; Luck, A.J.; Beard, H.; Hassiotis, S.; Mazouni, K.; Hopwood, J.J.; Kremer, E.J.; Hemsley, K.M. Helper-Dependent Canine Adenovirus Vector-Mediated Transgene Expression in a Neurodegenerative Lysosomal Storage Disorder. *Gene* **2012**, *491*, 53–57. [[CrossRef](#)]
76. Cardone, M.; Polito, V.A.; Pepe, S.; Mann, L.; D’Azzo, A.; Auricchio, A.; Ballabio, A.; Cosma, M.P. Correction of Hunter Syndrome in the MPSII Mouse Model by AAV2/8-Mediated Gene Delivery. *Hum. Mol. Genet.* **2006**, *15*, 1225–1236. [[CrossRef](#)]
77. Polito, V.A.; Cosma, M.P. IDS Crossing of the Blood-Brain Barrier Corrects CNS Defects in MPSII Mice. *Am. J. Hum. Genet.* **2009**, *85*, 296–301. [[CrossRef](#)]
78. Jung, S.-C.; Park, E.-S.; Choi, E.N.; Kim, C.H.; Kim, S.J.; Jin, D.-K. Characterization of a Novel Mucopolysaccharidosis Type II Mouse Model and Recombinant AAV2/8 Vector-Mediated Gene Therapy. *Mol. Cells* **2010**, *30*, 13–18. [[CrossRef](#)]
79. Hinderer, C.; Katz, N.; Louboutin, J.P.; Bell, P.; Yu, H.; Nayal, M.; Kozarsky, K.; O’Brien, W.T.; Goode, T.; Wilson, J.M. Delivery of an Adeno-Associated Virus Vector into Cerebrospinal Fluid Attenuates Central Nervous System Disease in Mucopolysaccharidosis Type II Mice. *Hum. Gene Ther.* **2016**, *27*, 906–915. [[CrossRef](#)]
80. Motas, S.; Haurigot, V.; Garcia, M.; Marcó, S.; Ribera, A.; Roca, C.; Sánchez, X.; Sánchez, V.; Molas, M.; Bertolin, J.; et al. CNS-Directed Gene Therapy for the Treatment of Neurologic and Somatic Mucopolysaccharidosis Type II (Hunter Syndrome). *JCI Insight* **2016**, *1*, e86696. [[CrossRef](#)]
81. Laoharawee, K.; Podetz-Pedersen, K.M.; Nguyen, T.T.; Evenstar, L.B.; Kitto, K.F.; Nan, Z.; Fairbanks, C.A.; Low, W.C.; Kozarsky, K.F.; Mcivor, R.S. Prevention of Neurocognitive Deficiency in Mucopolysaccharidosis Type II Mice by Central Nervous System-Directed, AAV9-Mediated Iduronate Sulfatase Gene Transfer. *Hum. Gene Ther.* **2017**, *28*, 626–638. [[CrossRef](#)] [[PubMed](#)]
82. Fu, H.; Zaraspe, K.; Murakami, N.; Meadows, A.S.; Pineda, R.J.; McCarty, D.M.; Muenzer, J. Targeting Root Cause by Systemic scAAV9-hIDS Gene Delivery: Functional Correction and Reversal of Severe MPS II in Mice. *Mol. Ther. Methods Clin. Dev.* **2018**, *10*, 327–340. [[CrossRef](#)] [[PubMed](#)]
83. Laoharawee, K.; DeKolver, R.C.; Podetz-Pedersen, K.M.; Rohde, M.; Sproul, S.; Nguyen, H.O.; Nguyen, T.; Martin, S.J.S.; Ou, L.; Tom, S.; et al. Dose-Dependent Prevention of Metabolic and Neurologic Disease in Murine MPS II by ZFN-Mediated In Vivo Genome Editing. *Mol. Ther.* **2018**, *26*, 1127–1136. [[CrossRef](#)]
84. Hordeaux, J.; Hinderer, C.; Goode, T.; Buza, E.L.; Bell, P.; Calcedo, R.; Richman, L.K.; Wilson, J.M. Toxicology Study of Intra-Cisterna Magna Adeno-Associated Virus 9 Expressing Iduronate-2-Sulfatase in Rhesus Macaques. *Mol. Ther. Methods Clin. Dev.* **2018**, *10*, 68–78. [[CrossRef](#)] [[PubMed](#)]
85. Wakabayashi, T.; Shimada, Y.; Akiyama, K.; Higuchi, T.; Fukuda, T.; Kobayashi, H.; Eto, Y.; Ida, H.; Ohashi, T. Hematopoietic Stem Cell Gene Therapy Corrects Neuropathic Phenotype in Murine Model of Mucopolysaccharidosis Type II. *Hum. Gene Ther.* **2015**, *26*, 357–366. [[CrossRef](#)]
86. Gleitz, H.F.; Liao, A.Y.; Cook, J.R.; Rowston, S.F.; Forte, G.M.; D’Souza, Z.; O’Leary, C.; Holley, R.J.; Bigger, B.W. Brain-targeted Stem Cell Gene Therapy Corrects Mucopolysaccharidosis Type II Via Multiple Mechanisms. *EMBO Mol. Med.* **2018**, *10*, e8730. [[CrossRef](#)]
87. Wada, M.; Shimada, Y.; Iizuka, S.; Ishii, N.; Hiraki, H.; Tachibana, T.; Maeda, K.; Saito, M.; Arakawa, S.; Ishimoto, T.; et al. Ex Vivo Gene Therapy Treats Bone Complications of Mucopolysaccharidosis Type II Mouse Models through Bone Remodeling Reactivation. *Mol. Ther. Methods Clin. Dev.* **2020**, *19*, 261–274. [[CrossRef](#)]
88. Miwa, S.; Watabe, A.M.; Shimada, Y.; Higuchi, T.; Kobayashi, H.; Fukuda, T.; Kato, F.; Ida, H.; Ohashi, T. Efficient Engraftment of Genetically Modified Cells Is Necessary to Ameliorate Central Nervous System Involvement of Murine Model of Mucopolysaccharidosis Type II by Hematopoietic Stem Cell Targeted Gene Therapy. *Mol. Genet. Metab.* **2020**, *130*, 262–273. [[CrossRef](#)]
89. Conway, A.; Mendel, M.; Kim, K.; McGovern, K.; Boyko, A.; Zhang, L.; Miller, J.C.; DeKolver, R.C.; Paschon, D.E.; Mui, B.L.; et al. Non-viral Delivery of Zinc Finger Nuclease mRNA Enables Highly Efficient In Vivo Genome Editing of Multiple Therapeutic Gene Targets. *Mol. Ther.* **2019**, *27*, 866–877. [[CrossRef](#)]
90. Josahkian, J.A.; Trapp, F.B.; Burin, M.G.; Michelin-Tirelli, K.; de Magalhães, A.P.P.S.; Sebastião, F.M.; Bender, F.; de Mari, J.F.; Brusius-Facchin, A.C.; Leistner-Segal, S.; et al. Updated Birth Prevalence and Relative Frequency of Mucopolysaccharidoses across Brazilian Regions. *Genet. Mol. Biol.* **2021**, *44*, 1–6. [[CrossRef](#)]
91. Diez-Roux, G.; Ballabio, A. Sulfatases and Human Disease. *Annu. Rev. Genom. Hum. Genet.* **2005**, *6*, 355–379. [[CrossRef](#)] [[PubMed](#)]
92. Poorthuis, B.J.H.M.; Wevers, R.A.; Kleijer, W.J.; Groener, J.E.M.; de Jong, J.G.N.; van Weely, S.; Niezen-Koning, K.E.; van Diggelen, O.P. The Frequency of Lysosomal Storage Diseases in The Netherlands. *Hum. Genet.* **1999**, *105*, 151–156. [[CrossRef](#)] [[PubMed](#)]
93. Kosuga, M.; Mashima, R.; Hirakiyama, A.; Fuji, N.; Kumagai, T.; Seo, J.-H.; Nikaido, M.; Saito, S.; Ohno, K.; Sakuraba, H.; et al. Molecular Diagnosis of 65 Families with Mucopolysaccharidosis Type II (Hunter Syndrome) Characterized by 16 Novel Mutations in the IDS Gene: Genetic, Pathological, and Structural Studies on Iduronate-2-Sulfatase. *Mol. Genet. Metab.* **2016**, *118*, 190–197. [[CrossRef](#)] [[PubMed](#)]

94. Sharma, R.; Anguela, X.M.; Doyon, Y.; Wechsler, T.; DeKolver, R.C.; Sproul, S.; Paschon, D.E.; Miller, J.C.; Davidson, R.J.; Shivak, D.; et al. In Vivo Genome Editing of the Albumin Locus as a Platform for Protein Replacement Therapy. *Blood* **2015**, *126*, 1777–1784. [[CrossRef](#)]
95. Cheng, M.H.Y.; Brimacombe, C.A.; Verbeke, R.; Cullis, P.R. Exciting Times for Lipid Nanoparticles: How Canadian Discoveries Are Enabling Gene Therapies. *Mol. Pharm.* **2022**, *19*, 1663–1668. [[CrossRef](#)]
96. Rurik, J.G.; Tombácz, I.; Yadegari, A.; Fernández, P.O.M.; Shewale, S.V.; Li, L.; Kimura, T.; Soliman, O.Y.; Papp, T.E.; Tam, Y.K.; et al. CAR T Cells Produced In Vivo to Treat Cardiac Injury. *Science* **2022**, *375*, 91–96. [[CrossRef](#)]
97. Hudry, E.; Vandenberghe, L.H. Therapeutic AAV Gene Transfer to the Nervous System: A Clinical Reality. *Neuron* **2019**, *101*, 839–862. [[CrossRef](#)]
98. Belur, L.R.; Romero, M.; Lee, J.; Podetz-Pedersen, K.M.; Nan, Z.; Riedl, M.S.; Vulchanova, L.; Kitto, K.F.; Fairbanks, C.A.; Kozarsky, K.F.; et al. Comparative Effectiveness of Intracerebroventricular, Intrathecal, and Intranasal Routes of AAV9 Vector Administration for Genetic Therapy of Neurologic Disease in Murine Mucopolysaccharidosis Type I. *Front. Mol. Neurosci.* **2021**, *14*, 618360. [[CrossRef](#)]
99. Bose, S.K.; White, B.M.; Kashyap, M.V.; Dave, A.; de Bie, F.R.; Li, H.; Singh, K.; Menon, P.; Wang, T.; Teerdhala, S.; et al. In Utero Adenine Base Editing Corrects Multi-Organ Pathology in a Lethal Lysosomal Storage Disease. *Nat. Commun.* **2021**, *12*, 4291. [[CrossRef](#)]
100. Riley, R.S.; Kashyap, M.V.; Billingsley, M.M.; White, B.; Alameh, M.G.; Bose, S.K.; Zoltick, P.W.; Li, H.; Zhang, R.; Cheng, A.Y.; et al. Ionizable Lipid Nanoparticles for In Utero mRNA Delivery. *Sci. Adv.* **2021**, *7*, eaba1028. [[CrossRef](#)]
101. Oller-Salvia, B.; Sánchez-Navarro, M.; Giralt, E.; Teixidó, M. Blood-Brain Barrier Shuttle Peptides: An Emerging Paradigm for Brain Delivery. *Chem. Soc. Rev.* **2016**, *45*, 4690–4707. [[CrossRef](#)] [[PubMed](#)]
102. Zhang, X.; Chai, Z.; Dobbins, A.L.; Itano, M.S.; Askew, C.; Miao, Z.; Niu, H.; Samulski, R.J.; Li, C. Customized Blood-Brain Barrier Shuttle Peptide to Increase AAV9 Vector Crossing the BBB and Augment Transduction in the Brain. *Biomaterials* **2022**, *281*, 121340. [[CrossRef](#)] [[PubMed](#)]
103. Antony, J.S.; Daniel-Moreno, A.; Lamsfus-Calle, A.; Raju, J.; Kaftancioglu, M.; Ureña-Bailén, G.; Rottenberger, J.; Hou, Y.; Santhanakumaran, V.; Lee, J.H.; et al. A Mutation-Agnostic Hematopoietic Stem Cell Gene Therapy for Metachromatic Leukodystrophy. *Cris. J.* **2022**, *5*, 66–79. [[CrossRef](#)] [[PubMed](#)]
104. Pavel-Dinu, M.; Wiebking, V.; Dejene, B.T.; Srifá, W.; Mantri, S.; Nicolas, C.E.; Lee, C.; Bao, G.; Kildebeck, E.J.; Punjya, N.; et al. Gene Correction for SCID-X1 in Long-Term Hematopoietic Stem Cells. *Nat. Commun.* **2019**, *10*, 1634. [[CrossRef](#)] [[PubMed](#)]
105. Rai, R.; Romito, M.; Rivers, E.; Turchiano, G.; Blattner, G.; Vetharoy, W.; Ladon, D.; Andrieux, G.; Zhang, F.; Zinicola, M.; et al. Targeted Gene Correction of Human Hematopoietic Stem Cells for the Treatment of Wiskott-Aldrich Syndrome. *Nat. Commun.* **2020**, *11*, 4034. [[CrossRef](#)]
106. Tran, N.T.; Graf, R.; Wulf-Goldenberg, A.; Stecklum, M.; Strauß, G.; Kühn, R.; Kocks, C.; Rajewsky, K.; Chu, V.T. CRISPR-Cas9-Mediated ELANE Mutation Correction in Hematopoietic Stem and Progenitor Cells to Treat Severe Congenital Neutropenia. *Mol. Ther.* **2020**, *28*, 2621–2634. [[CrossRef](#)]